







## Fully coupled hydrological–hydrodynamic modeling of a basin–river–lake transboundary system in Southern South America

Thais Magalhães Possa <sup>a,\*</sup>, Gilberto Loguercio Collares <sup>b</sup>, Lukas dos Santos Boeira <sup>b</sup>,  
Pedro Frediani Jardim <sup>a</sup>, Fernando Mainardi Fan <sup>a</sup> and Viviane Santos Silva Terra <sup>b</sup>

<sup>a</sup> Instituto de Pesquisas Hidráulicas, Universidade Federal do Rio Grande do Sul (UFRGS), Av. Bento Gonçalves, 9500, Porto Alegre, Rio Grande do Sul 91501-970, Brazil

<sup>b</sup> Engenharia Hídrica/Centro de Desenvolvimento Tecnológico, Universidade Federal de Pelotas, Gomes Carneiro, 01, Pelotas, Rio Grande do Sul 96010-610, Brazil

\*Corresponding author. E-mail: thaispossa03@gmail.com

 TMP, 0000-0001-5221-8755; GLC, 0000-0003-4910-5420; L dos SB, 0000-0002-6139-5750; PFJ, 0000-0002-7192-8370; FMF, 0000-0003-0371-7851; VSST, 0000-0002-9020-3148

### ABSTRACT

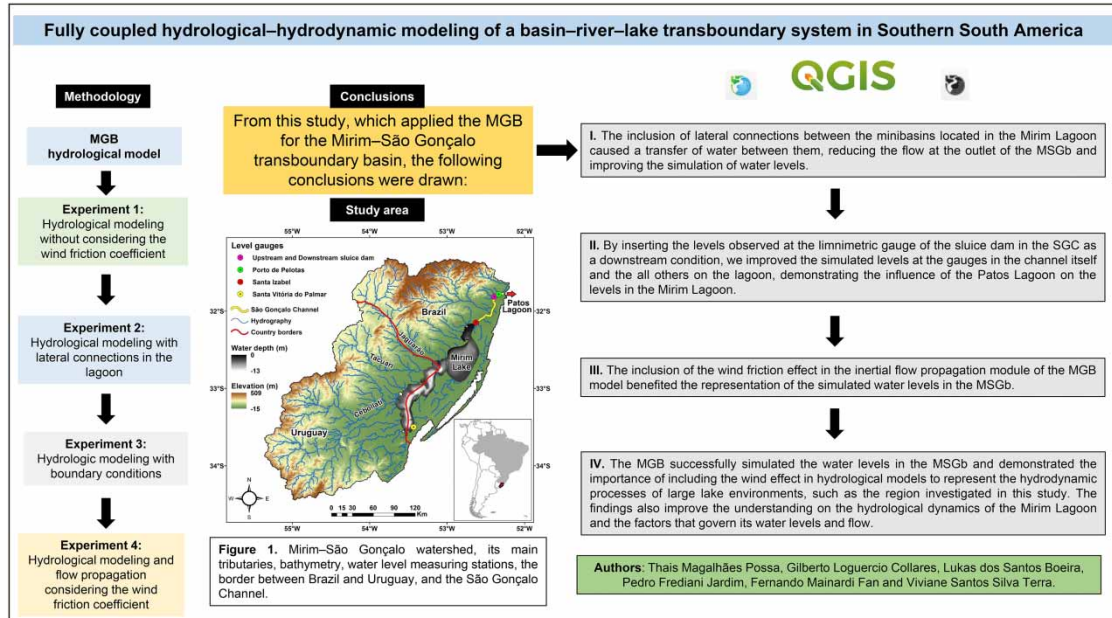
The Mirim and Patos Lagoons form the largest lagoon complex in South America. Wind is one of the dominant climatic elements of circulation and water levels in the basin. Therefore, we aimed to better understand the effects of wind on the Mirim–São Gonçalo watershed by applying the MGB hydrological model and to assess whether it would produce satisfactory results for modeling. Various tests were performed to determine the best representation of the processes involved and the observed levels. The best results were obtained with the inclusion of sub-daily wind data in the simulation and also the downstream boundary condition by using the observed water level data at the sluice dam of the São Gonçalo channel. The results showed that the model could successfully simulate the levels and demonstrated the importance of including the wind when modeling the hydrodynamic processes of large lake environments.

**Key words:** hydrological–hydrodynamic modeling, large-scale modeling, MGB, Mirim Lagoon

### HIGHLIGHTS

- What is the numerical effect of introducing wind influence in the inertial flux propagation method?
- What are the optimal values of the coefficient of wind friction and parameterization for minibasin connections to obtain the best simulation of the lagoon?
- Does the inclusion of lock level information in the SGC as a downstream boundary condition and hourly winds benefit the level representation?

## GRAPHICAL ABSTRACT



## NOTATION

|       |   |
|-------|---|
| MSGb  | Mirim–São Gonçalo basin                           |
| SGC   | São Gonçalo channel                               |
| DEM   | Digital Elevation Model                           |
| SRTM  | Shuttle Radar Topography Mission                  |
| HRUs  | Hydrologic Response Units                         |
| INMET | National Meteorological Institute                 |
| ANA   | National Water Agency                             |
| ALM   | Mirim Lagoon Development Agency                   |
| HAND  | Height Above Nearest Drainage                     |
| $C_d$ | wind friction coefficient                         |
| NS    | Nash–Sutcliffe coefficient                        |
| NSlog | Nash–Sutcliffe coefficient of the flow logarithms |
| Bias  | relative volume error                             |
| RMSE  | Root Mean Square Error                            |
| S-DW  | Sub-Daily Wind                                    |
| HW    | Hourly Wind                                       |
| B     | Width of lateral connections                      |

## INTRODUCTION

Hydrological models have been widely used in studies on hydrological forecasting (e.g., Fan *et al.* 2016), impacts associated with climate change (e.g., Sorribas *et al.* 2016; Amorim & Chaffe 2019; Brêda *et al.* 2020; Schuster *et al.* 2020) and land use (e.g., Kundu *et al.* 2017), mapping areas with flood risks (e.g., Komi *et al.* 2017), representing the generation and propagation of runoff in rivers and other processes of the hydrological cycle (e.g., Fan *et al.* 2014) and water quality (e.g., Moriasi *et al.* 2015; Pinaridi *et al.* 2015).

In this sense, authors have been dedicating themselves to the collection and generation of relevant information for hydrological modelings, such as precipitation estimations based on satellite products (Abdelmoneim *et al.* 2020; Sharannya *et al.* 2020) or even variables like the average temperature of the surface and wind speed from meteorological reanalysis products (Valipour *et al.* 2021).

Recent advances in large-scale hydrological–hydrodynamic modeling have enabled the simulation of runoff in basins with extensive river networks and water bodies such as lakes and lagoons, with the aim of predicting short-term water levels, studying circulation, assessing climate change and its effects on flooded areas, etc. (Lian *et al.* 2007; Paz *et al.* 2010; Fragoso *et al.* 2011).

The standard approach to simulating these complex water systems involves externally coupling a hydrological model to a two- or three-dimensional hydrodynamic model. In this coupling, the output data of the hydrological model serves as the input of the hydrodynamic model of the lake or pond (Dargahi & Setegn 2011; Li *et al.* 2014).

Examples of this coupling approach between river basin and lake models include the Hydrological Model of Large Basins (MGB) large-scale hydrological model (Collischonn *et al.* 2007; Pontes *et al.* 2017), the large basins model, and the three-dimensional hydrodynamic and ecological model IPH-ECO (Fragoso *et al.* 2009). Munar *et al.* (2018) applied the MGB outputs to the hydrodynamic model to simulate the Mirim–São Gonçalo basin (MSGb), located in the extreme south of Brazil, and validated the application using *in situ* observed data and satellite altimetric data.

The Mirim Lagoon is connected to the Patos Lagoon through the São Gonçalo channel (SGC), and its waters are significant to the key economic activities in the region, such as fishing, livestock uses, and rice farming (Kunz & Castrogiovanni 2020). In flood events, the Mirim Lagoon can connect to the Mangueira Lagoon through wetlands, forming the largest lagoon complex in South America (Kjerfve 1986) and its dynamics depend on wind and freshwater discharge (Möller *et al.* 2001; Oliveira *et al.* 2015). It is because of the wind effect that the flows and levels constantly vary over time, which is considered a key factor in the system (Ji 2008).

Some hydrodynamic studies on the Mirim Lagoon analyzed the effects of these factors on various activities (navigation and transport of pollutants). Oliveira *et al.* (2019) used the three-dimensional hydrodynamic circulation model TELEMAC-3D (Hervouet 2007) and observed that prevailing winds in the S-SW directions can generate adverse conditions for navigation as they create shallow regions in the lagoon. Using a series of discharge and reanalysis of atmospheric data and the two-dimensional model TELEMAC-2D, Silva *et al.* (2019) simulated the transport patterns and residence time of the Mirim Lagoon and verified a high variability in the distribution of residence time in the lagoon owing to wind and discharge conditions, which determines the greater susceptibility of pollutant transport in specific periods.

In the Patos Lagoon basin, integrated approaches of hydrological–hydraulic models have also been applied to deepen the understanding of the local hydrodynamics, although only in few studies. In these studies, the flow rates of the main tributaries to the lagoons were used as the boundary conditions, calculated using estimates from the historical series of fluvimetric and limnometric stations (e.g., Möller *et al.* 1996, 2001; Marques & Möller 2008; Barros *et al.* 2014; Cavalcante & Mendes 2014).

Based on this, Lopes *et al.* (2018) proposed an integrated approach by including the wind shear stress in the MGB hydrological model to simulate the flows, water levels, and flooded areas in the Patos Lagoon basin. They concluded that the proposed model obtained good results which can be used to simulate flood forecasting systems and other similar hydrological systems.

However, for the MSGb, the available literature has not considered integrated hydrological–hydrodynamic modeling that includes the effects of wind on water levels and the evaluation of flooded areas using the model.

Munar *et al.* (2018) has adopted the offline coupling between the MGB model and the hydrodynamic model IPH-ECO. The authors obtained good performance on the representation of water levels for some of the gauges presented in this study. In this case, the hydrodynamic uses the hydrological–hydraulic model outputs as input. However, this is a costly approach and requires more processing time. In addition, since the models run sequentially, backwater effects between rivers and lakes are hardly represented, and therefore, the hydrodynamic model does not influence the hydrological–hydraulic model (Li *et al.* 2014). Thus, the present study aims to fill this gap, presenting an integrated model or ‘full coupling’ that better represents the water levels along the Lagoon, as well as analyzing the influence of the wind in the lagoon region with a single model, which allows the use of propagation modules for the entire modeled system.

Thus, in this study, we addressed this by answering four questions:

1. Can the MSGb, including its lakes, be simulated to estimate water levels and flooded areas using the framework of a large-scale hydrological–hydraulic model?
2. What is the numerical effect of introducing the wind influence into the inertial flow propagation method?
3. What are the optimal values of the wind friction coefficient ( $C_d$ ) and parameterization for minibasin connections to obtain the best simulation of the lagoon?

4. Does including the wind variable in the large-scale hydrological–hydraulic model benefit the representation of simulated water levels of the MSGb?
5. Does the inclusion of level information from the sluice dam in the SGC as a downstream boundary condition and hourly winds benefit the representation of levels in the configurations tested in this study?

Four experiments were conducted to answer these questions. The first involved performing the modeling in its typical form, i.e., without modifications. The second involved the methodology of inserting effective channels between all adjacent mini-basins located in lagoon areas to connect them. In the third one, different downstream boundary conditions were used: (i) a constant slope condition of  $0.5 \text{ m km}^{-1}$ , (ii) a constant sea level, and (iii) daily water level data, observed at the downstream gauge at the SGC dam. In the fourth experiment, two analyses were performed, one using the sub-daily data and the other using hourly data considering in both cases the information from the sluice dam at SGC as a downstream boundary condition, as the best-simulated levels were observed with this strategy.

### Case study

The MSGb is located between the coordinates  $31^{\circ}30'$  to  $34^{\circ}35'$  South and  $53^{\circ}31'$  to  $55^{\circ}15'$  West, with an area of approximately  $62,250 \text{ km}^2$ , of which  $29,250 \text{ km}^2$  (47%) lies in the Brazilian territory and  $33,000 \text{ km}^2$  (53%) in the Uruguayan territory (Sosinski 2009).

The digital elevation model (DEM) of the basin derived from Shuttle Radar Topography Mission (SRTM) data (Farr *et al.* 2007) varies over a wide range of values, with elevations reaching 509 m in mountainous areas and approximately 0 a.s.l. in the floodplain areas around the Mirim Lagoon. The main tributaries of the Mirim Lagoon are the Jaguarão and Piratini rivers on the Brazilian side and the Cebollati and Tacuarí rivers on the Uruguayan side. The northern sector of the lagoon, between the Tacuarí river and the SGC, has approximately 3 m deep, making it shallow and wide compared with the other regions which are approximately 8 m deep and narrower (Figure 1; Silva *et al.* 2019).

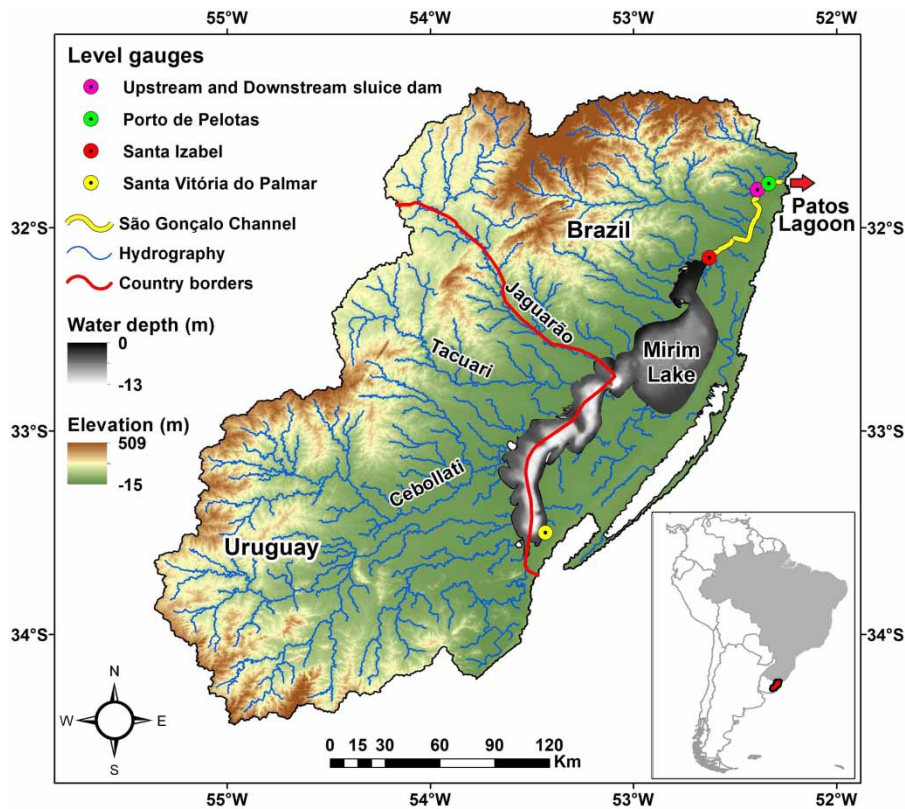


**Figure 1** | Mirim–São Gonçalo watershed, its main tributaries, bathymetry, water level measuring stations, the border between Brazil and Uruguay, and the São Gonçalo channel.



The Mirim Lagoon has an approximate length of 190 km along the major axis, an average length of 40 km in its widest portion, and 20 km in the narrowest portion. Its volume can reach 12.4 billion m<sup>3</sup> and varies depending on the flow and hydrological conditions (Kotzian & Marques 2004).

Considered the second largest coastal lagoon in Brazil, the Mirim Lagoon, together with the Patos Lagoon, forms the largest lagoon complex in South America (Oliveira *et al.* 2015). The waters of the Mirim Lagoon flow through the SGC, a 76.6 km long channel that has a lock–dam system at its northeast end, preventing the intrusion of saline water during the dry season and maintaining the lagoon’s volume (Vieira 1988).

## MATERIALS AND METHODS

In this study, we used the MGB version of the hydrological model presented by Pontes *et al.* (2017) and Lopes *et al.* (2018). The methodology described by Pontes *et al.* (2017) was adopted for minibasins in lagoon areas. The model was modified with the inclusion of the downstream condition of the CSG sluice dam and the introduction of a new dataset with a series of sub-daily and hourly wind direction and speed in the simulations. The data required for modeling are described below.

### Data used

The input data were obtained through the DEM of the SRTM, which has a spatial resolution of 90 m and a vertical resolution of 1 m (Farr *et al.* 2007). Despite the errors and limitations of SRTM due to problems in the reflection of radar signals in water bodies or on steep slopes (Farr *et al.* 2007), its use was still suitable for the proposed modeling, and it has been widely tested in previous studies (Paz *et al.* 2008).

The bathymetry of the Mirim Lagoon was extracted from the Brazilian Navy’s hydrography and navigation chart that contains data before the year 1941 and it was inserted in the DEM, enabling the representation of the lagoon bathymetry in the model.

Soil and land use information for the basin was obtained using a map of hydrologic response units (HRUs) developed by Fan *et al.* (2015), available for South America (<https://www.ufrgs.br/lsh/products/simplified-hydrologicalresponse-unidades-mapa-para-américa-south/>). Each HRU has a hydrological behavior, which directly affects the hydrological processes simulated by the model.

Meteorological data such as air temperature, air humidity, atmospheric pressure, and insolation were obtained from the internal database of the MGB model, which contains a set of climatological normals from 1960 to 1990, calculated by the National Meteorological Institute (INMET) of Brazil (Fan & Collischonn 2014). These data were used to obtain evapotranspiration values using the Penman–Monteith method (Allen *et al.* 1998) in the HRUs of each watershed.

Daily hydrological data from 91 pluviometric gauges and 14 fluviometric gauges were also used, of which 8 fluviometric and 45 pluviometric gauges were provided by the meteorological authorities of the Uruguayan territory and the remainder by the national hydrological network managed by the National Water Agency (ANA) of Brazil.

In the survey of the limnimetric data, 10 gauges were identified in the MSGb (Figure 1), of which five belong to the ANA database. The water level data from the gauges in Santa Isabel, Santa Vitória do Palmar, and upstream and downstream of the SGC dam were obtained from the Mirim Lagoon Development Agency (ALM) of the Federal University of Pelotas. The water levels of the SGC were provided by the Port of Pelotas, which has a ruler installed next to the pier.

### Hydrological and hydrodynamic model

The MGB model is a process-based semi-distributed rainfall–runoff model developed for the simulation of large watersheds. The model was first introduced by Collischonn *et al.* (2007) and subsequently improved by Paiva *et al.* (2011), Pontes *et al.* (2017), and Fleischmann *et al.* (2018).

It was first used in large basins in South America, for example, to assess climate change impacts in the Amazon (Sorribas *et al.* 2016), in hydrological and hydrodynamic modeling of rivers and lakes (Lopes *et al.* 2018; Munar *et al.* 2018; Fleischmann *et al.* 2019a, 2019b), in water management scenarios in transboundary river basins (Gorgoglione *et al.* 2019), and in continental hydrological modeling for South America (Siqueira *et al.* 2018).

In its most recent version, the drainage network is extracted from a high-resolution DEM using a vector-based approach and the basin is discretized into minibasins (Figure 2(b)), each containing a river segment with a constant length and a flood-plain associated with a vertical water and energy balance (Siqueira *et al.* 2016). The basin is also subdivided into sub-basins

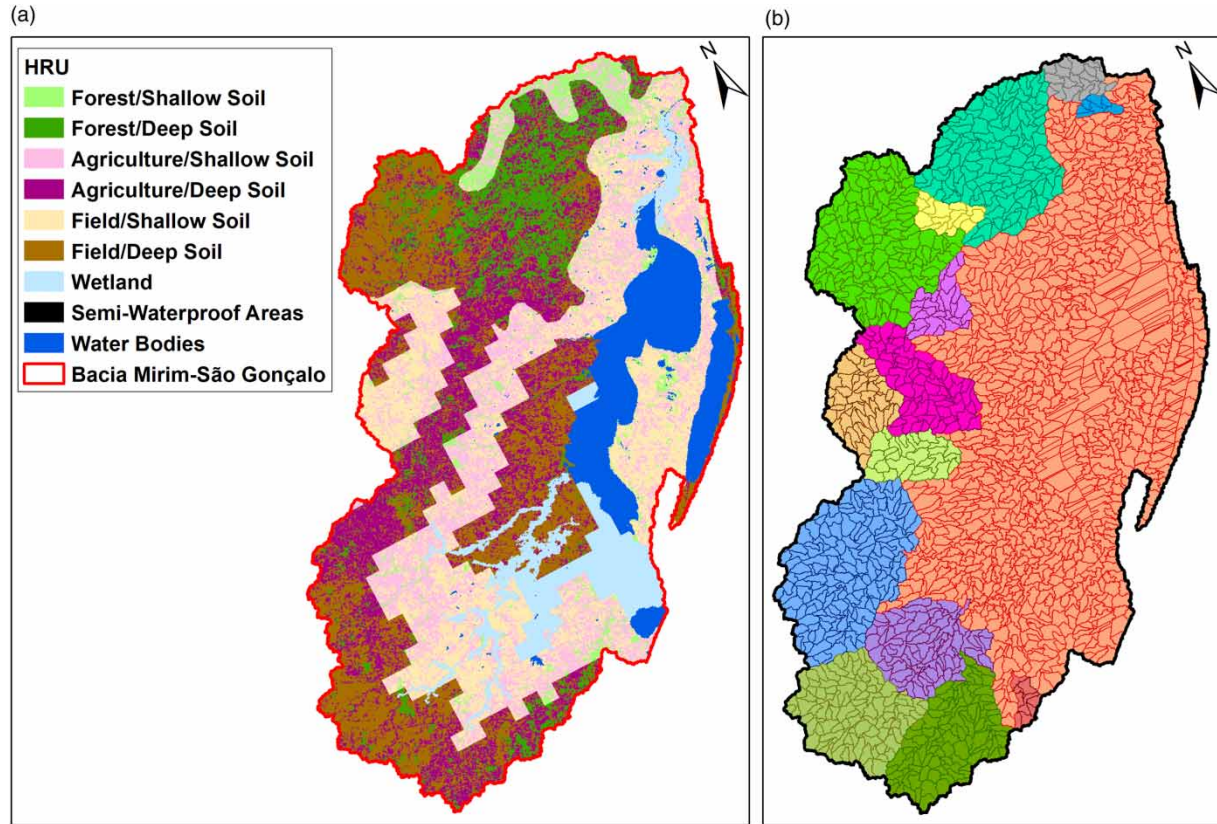


**Figure 2** | (a) Map of response units (HRU) used to simulate each hydrologic process within a watershed. (b) Discretization into 15 sub-basins used to define model parameters and 1,777 minibasins.

(Figure 2(b)), defined as macro drainage areas that encompass many minibasins with the same model parameter values. The MSGb was discretized into 15 sub-basins and 1,777 minibasins, each one associated with a river reach of 10 km.

In addition to the discretization into sub-basins and minibasins, the basin was subdivided into HRUs, resulting from the combination of land use and soil type maps (Figure 2(a)), and for each of them, the model simulated the vertical water and energy balance, evapotranspiration, and the generation of surface, subsurface, and subsurface runoff. The water and energy balance were calculated through the soil-vegetation system. The runoff volumes in each HRU within each minibasin were stored in simple linear reservoirs and routed to the river network using the Muskingum-Cunge method or one-dimensional (1D) hydrodynamic equations (Pontes *et al.* 2017).

The representation of flow propagation in the rivers of the MSGb was performed using 1D hydrodynamic equations, based on a simplification of the Saint-Venant equations, constituted by the continuity equation (Equation (1)) and momentum conservation (Equation (2)):

$$\frac{\partial A}{\partial t} + \frac{\partial Q}{\partial x} = q \quad (1)$$

$$\frac{\partial Q}{\partial t} + \frac{\partial \left( \frac{Q^2}{A} \right)}{\partial x} + g \cdot A \cdot \frac{\partial h}{\partial x} + g \cdot A \cdot S_f = 0 \quad (2)$$

where  $Q$  is the flow rate ( $\text{m}^3 \text{s}^{-1}$ ),  $A$  is the cross-sectional area of the flow ( $\text{m}^2$ ),  $x$  is the distance in the longitudinal direction (m),  $t$  is the time (s), and  $g$  is the acceleration of gravity ( $\text{m s}^{-2}$ ).

To solve Equation (2), we used the local explicit inertial method proposed by Bates *et al.* (2010), successfully tested in recent MGB applications (Pontes *et al.* 2017; Fleischmann *et al.* 2018). In this study, we used the version of the MGB

hydrological model presented by Pontes *et al.* (2017) and Lopes *et al.* (2018), including lateral flow exchanges between minibasins with areas defined as lowland and the wind friction coefficient in Equation (2) of the 1D hydrodynamic equations.

## Experiments

The methodology was based on four experiments performed sequentially, each assuming the best results of the previous one to represent the simulated water levels. The first experiment involved performing the modeling in its primitive form, i.e., without modifications of the other experiments available, such as the insertion of lateral connections in the minibasins located in the Mirim lagoon, incorporation of the downstream condition, and a new dataset with a series of directions and speeds of the sub-daily and hourly wind in the simulations. The main results generated by the MGB model are presented in the form of hydrographs, waveforms, and objective functions.

### Experiment 1: hydrological modeling without considering the wind friction coefficient

The model was calibrated using precipitation and river flow data from January 1, 1990 to December 31, 2015. The modeling was improved through manual calibration, by trial and error, to obtain a better agreement between the simulated and observed hydrographs, and by the adjustment of the objective functions.

### Experiment 2: hydrological modeling with lateral connections in the lagoon

In this experiment, the methodology of Pontes *et al.* (2017) was adopted in the MGB model to better represent the ponds and floodplains of the basin. According to the authors, it can be performed by incorporating effective channels between all adjacent minibasins located in lowland areas and thus connecting them. Therefore, the minibasins that are in the plain area and within the lagoon were identified, where, although there are no river stretches, water is still transferred freely between them. The length of the effective channels was calculated by summing the radius of two circles with areas equivalent to the ones of the two connected minibasins. The width (parameter  $b$ ) was defined as 100 m using a sensitivity analysis with different values of  $b$  to determine the effect of changes on the value of the objective functions obtained at level gauges near the Mirim Lagoon, these being 10, 100, 250, 500, and 1,000 m.

### Experiment 3: hydrologic modeling with boundary conditions

In this test, the objective functions obtained at level gauges near the Mirim Lagoon and the inundation maps in dry and flood periods were compared using different downstream boundary conditions: (i) constant slope condition of  $0.5 \text{ m km}^{-1}$ , (ii) a constant sea level, and (iii) daily water level data, observed at the downstream gauge of the sluice dam of the SGC. The inundated areas were estimated in a distributed manner along the basin using the height above nearest drainage (HAND) terrain model (Rennó *et al.* 2008; Nobre *et al.* 2011) and validated using the Global Surface Water product, produced through the analysis of 3 million images from the Landsat satellite at 30 m resolution over the last 32 years (Pekel *et al.* 2016).

### Experiment 4: hydrological modeling and flow propagation considering the wind friction coefficient

In this study, two analyses were performed, one using sub-daily wind data and another using hourly data, both considering the information from the sluice dam of the SGC, as a downstream boundary condition because the best-simulated levels were observed with the use of these in Experiment 3. The datasets of wind speed and direction were obtained through the meteorological gauges identified in Figure 3.

The sub-daily dataset is composed of three daily measurements at 00:00, 12:00, and 18:00 UTC but has gaps in 2015 for the Rio Grande gauge and between the years 1990 and 1992 for all stations. The hourly wind information has a lower data amount compared with the sub-daily data, starting only in the mid-2000s. They were interpolated from the meteorological stations to the locations of the centroids of each minibasin of the model using the nearest neighbor method.

To incorporate the frictional force that the wind exerts on the hydric system, the wind stress was considered to be tangential to the force acting on the water surface, and this is represented as Equation (3) (Ji 2008):

$$\tau = d_{ar} \cdot C_d \cdot |U| \cdot U \quad (3)$$

where  $\tau$  is the stress caused by the wind in the flow,  $U$  is the value of the wind velocity vector component in the flow direction ( $\text{m s}^{-1}$ ),  $d_{ar}$  is the air density ( $\text{kg m}^{-3}$ ), and  $C_d$  is the wind friction coefficient (dimensionless).

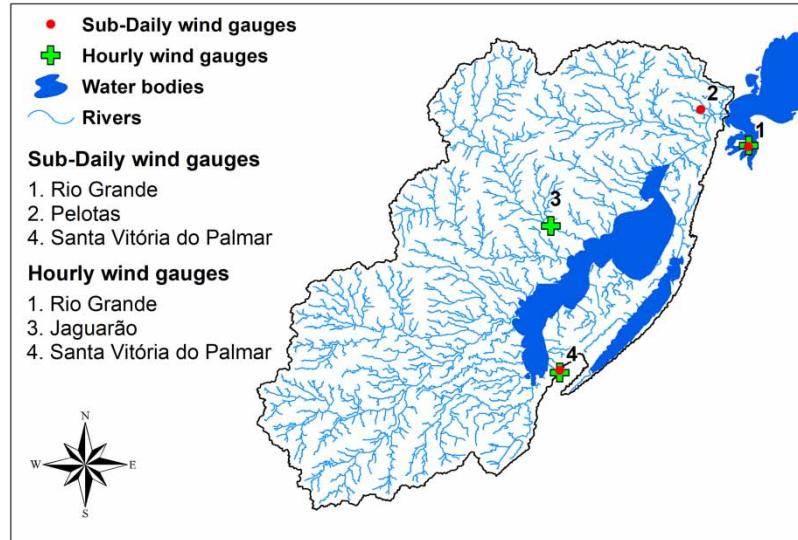


**Figure 3** | Meteorological posts located in the study area with wind data.

The wind velocity ( $U$ ) was multiplied by its modulus to preserve its direction (against or in favor of the flow). The inclusion of the wind tension force in the MGB model was performed by [Lopes et al. \(2018\)](#) through the modification of the dynamic equation of the inertial model (Equation (4)):

$$Q_i^{t+\Delta t} = \frac{((Q_i^t) - g \cdot B \cdot \Delta t \cdot (h_{\text{flow}i} \cdot S_{\text{flow}i}) + \Delta t \cdot B \cdot d_{ar} \cdot C_d \cdot |U| \cdot U)(-\cos(Azv_i - Azm_i))}{\left(1 + \frac{g \cdot \Delta t \cdot (|Q_i^t|) \cdot n^2}{B + (h_{\text{flow}})^3}\right)} \quad (4)$$

where  $Azv_i$  is the azimuth of wind direction in minibasin  $i$ , and  $Azm_i$  is the azimuth equivalent to the imaginary line that connects the centroids of the upstream ( $i$ ) and downstream ( $i + 1$ ) minibasins, defining the direction of flow.

The main associated modification corresponds to the introduction of the term  $-\cos(Azv_i - Azm_i)$ , which represents the decomposition of the wind velocity vector in the flow direction. For the application of Equation (4), it was necessary to apply a sensitivity test, running the model during the calibration period (1990–2015) using different values for parameter  $C_d$ :  $2 \times 10^{-6}$ ,  $4 \times 10^{-6}$ ,  $10 \times 10^{-6}$ , and  $20 \times 10^{-6}$ .

The effect of the coefficient value in the simulation of water levels was verified by comparing the objective functions in level gauges near the Mirim Lagoon, including in the model with sub-daily (three times a day) wind data from conventional gauges and hourly from automatic gauges, enabling the comparison of the simulated levels with each dataset. For these simulations, the performance metrics were evaluated and compared with the results obtained in Experiment 3.

Concerning the wind distribution in the model, for each timestep simulated wind data were obtained at each minibasin using the nearest gauge with hour information. In the case of none of the gauges had data for the specific timestep, then the model was applied as if the wind speed was zero. Regarding sub-daily gauges, to fill in the missing hours, linear equations were applied between the available speed data at each 3 h and the directions information was repeated between those 3 h in order to have data for every hour in the simulation.

### Objective functions used as performance metrics of the simulated levels

The objective functions used in the calibration were the Nash–Sutcliffe coefficient (NS), the NS coefficient of the flow logarithms (NSlog), and the relative volume error (Bias). The adjustments of water levels of the four experiments were verified using the NS, NSlog, and root mean square error (RMSE) functions and visually using the cotagrams in the five limnometric gauges near the Mirim Lagoon. Since the zero references of the model is different from that of the limnometric gauges,



the simulated water levels were adjusted to the observed reference using the average of the observed series for the same period. These specific metrics were used because they are the most frequently used in studies involving the MGB.

## RESULTS AND DISCUSSIONS

### Experiment 1

The results of the model calibration will be represented using (i) hydrograms of the observed and simulated flows, (ii) maps in which the fluvimetric posts used in the calibration are colored according to the value of the model performance metrics, and (iii) cotagrams of observed and simulated water levels and objective functions presented at the limnometric posts of the Mirim Lagoon.

### Simulated flow calibration results

In general, the model had a good performance, with the NS greater than 0.5 for most posts. These are, on the Uruguayan side, *Puente Ruta 8* (Vieja), *Picada de Corbo*, *Paso Borches*, and *Paso Dragon*, and on the Brazilian side, *Picada da Areia*, *Pedro Osório*, *Passo dos Carros*, and *Ponte Cordeiro de Farias* (Figure 4).

At the *Vergara*, *India-Muerta*, *Puente R.13*, *Passo Del Avestruz*, and *Passo Averías* stations, located in Uruguay, the model exhibited a low performance regarding peak flows, with good results only in the simulation of base flows at the *Vergara* and *Passo Del Avestruz* gauges (Figure 4). This may be associated with the lower resolution of the HRU map in the Uruguayan region (Figure 2(a)) or with the lower availability of data from rainfall gauges at the region.

The model exhibited a good performance in the NSlog metric at most of the gauges (more than 60%) of the MSGb, with average values of 0.58. The results were better than the NS values and indicated a good adjustment of the minimum flows. We observed that the model generally exhibited acceptable volume errors. The best results were values between  $-10$  and  $10\%$ . The largest volumetric errors occurred in the Uruguayan portion of the basin (Figure 4).

In relation to the observed and simulated hydrographs in the Uruguayan portion of the basin, in the Olimar Grande river, there was an underestimation of peak flows, although it had good agreement with the baseflows (Figure 5(a)). The peaks of the simulated hydrograms of the Cebollatí river were underestimated compared with the observed ones (Figure 5(b) and 5(c)). Additionally, we observed that in the recession periods, the model represented satisfactory through calibration, which demonstrated its good performance in the simulation of minimum flows.

The observation of the hydrographs also indicates that at the *Picada de Corbo* fluvimetric gauge, the MGB model better represented the hydrological regime (Figure 5(b)), both for peak and base flows, when compared with the hydrograph at the *Paso Averías* gauge in the same calibration period, reflecting better NS and NSlog indexes (Figure 5(c)). The gauge located in the Tacuarí river exhibited similar behavior, and an excellent correlation was observed between observed and simulated data (Figure 5(d) and 5(e)).

Overall, the model obtained a good representation during most of the simulated period in the Olimar Grande, Cebollatí, and Tacuarí rivers. However, on some dates, there was less volume during peak flows which may have occurred due to the lack of temporal and spatial rainfall data or to the lowest resolution of the hydrological response units (HRU) map in the southern region of the basin, in the Uruguayan portion. In addition, there could be incorrect fluvimetric data in the region. Also, in the southern region, there are plains portions, which are more difficult to calibrate and represent.

In the Brazilian portion of the basin, where the main tributaries are the Piratini and Jaguarão rivers, the observation of the hydrographs indicated that the peak flow was underestimated and that the rise was typically faster than the recession (Figure 6). In contrast, we observed that even with the scarcity of rainfall data in the region, the model satisfactorily represented the flows in dry periods with a reasonable agreement between the simulated and observed hydrographs.

The Piratini river flows into the SGC and is considered one of the main control elements as the channel flows toward the Patos Lagoon (Hartmann & Harkot 2018). Although, in some instances, the peak flows were underestimated by the model, a good correlation was observed between the observed and simulated values as indicated by the NS and NSlog metrics.

### Results of simulated water levels

The values of the performance metrics (NS, NSlog, and RMSE) used to evaluate the anomalies between the simulated and observed water level at each gauge in Experiment 1 indicates that the model correctly represented water levels at certain locations and poorly at others (Table 1).

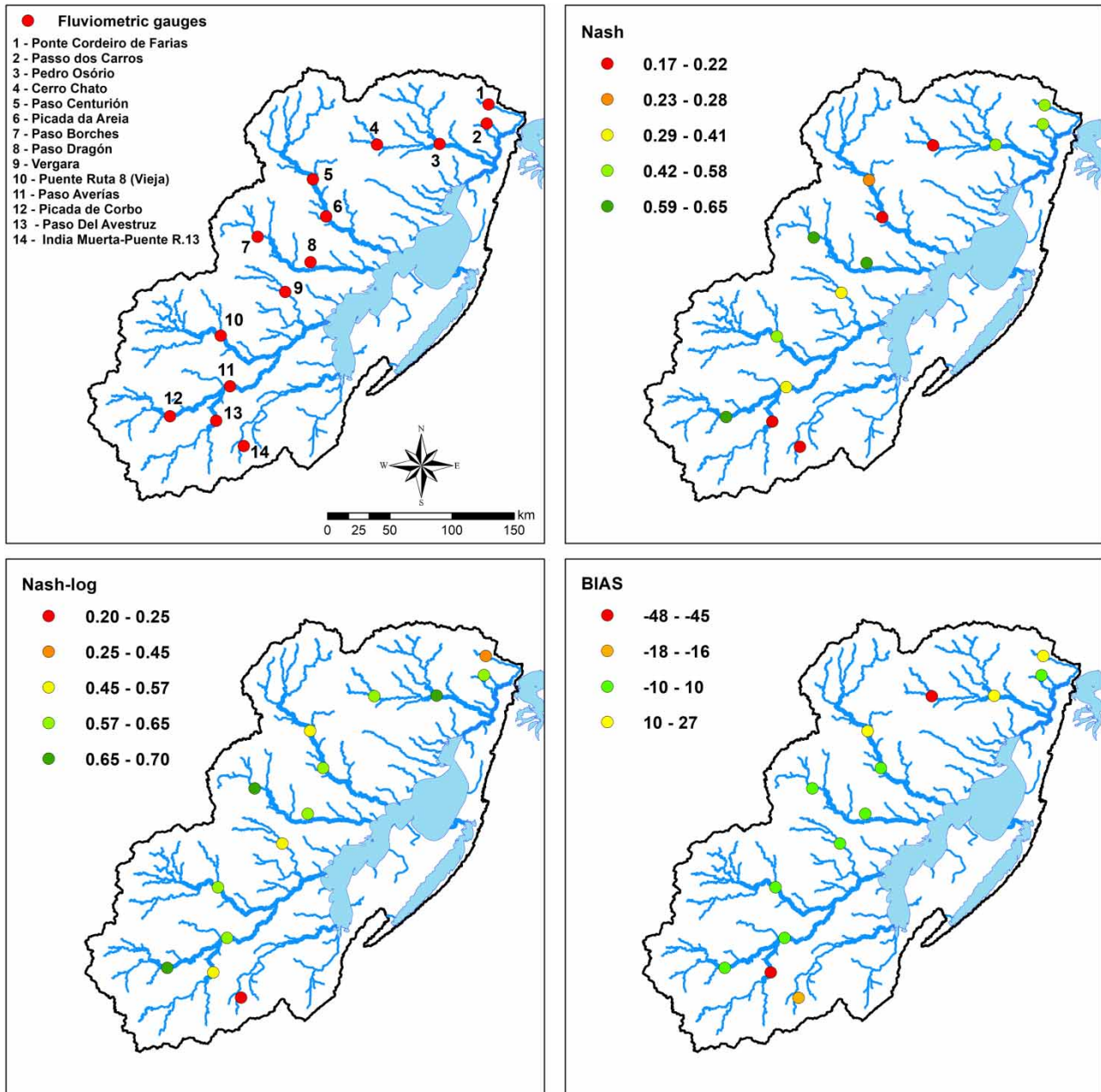


**Figure 4** | Calibration of NS, NSlog and volume error (absolute Bias) results.

The best NS values oscillated around 0.7 at the *Santa Isabel* and *Santa Vitória do Palmar* gauges. The unsatisfactory results obtained at the other gauges are associated with the absence of the operation of the Sluice Dam in the model, as well as the representation of the hydrodynamics of the Mirim Lagoon, such as the effects of wind and interaction with the Patos Lagoon. The best NSlog result was observed at the *Santa Isabel* gauge. The RMSE values ranged from 0.53 m in the location of the *Santa Vitória do Palmar* gauge to 0.32 m in *Porto de Pelotas*.

As shown in Table 1, the simulated levels at the *Santa Isabel* and *Santa Vitória do Palmar* gauges had a good representation of the observed levels observing the anomalies between them. In the same way as in the flows, during the flood period most of the extreme events were underestimated, except for *Porto de Pelotas*.

The level data from the gauges downstream and upstream of the sluice dam of the SGC and the *Port of Pelotas* exhibited strong vibrations, which suggests the inability of the model to simulate high-frequency oscillations of the water levels. These

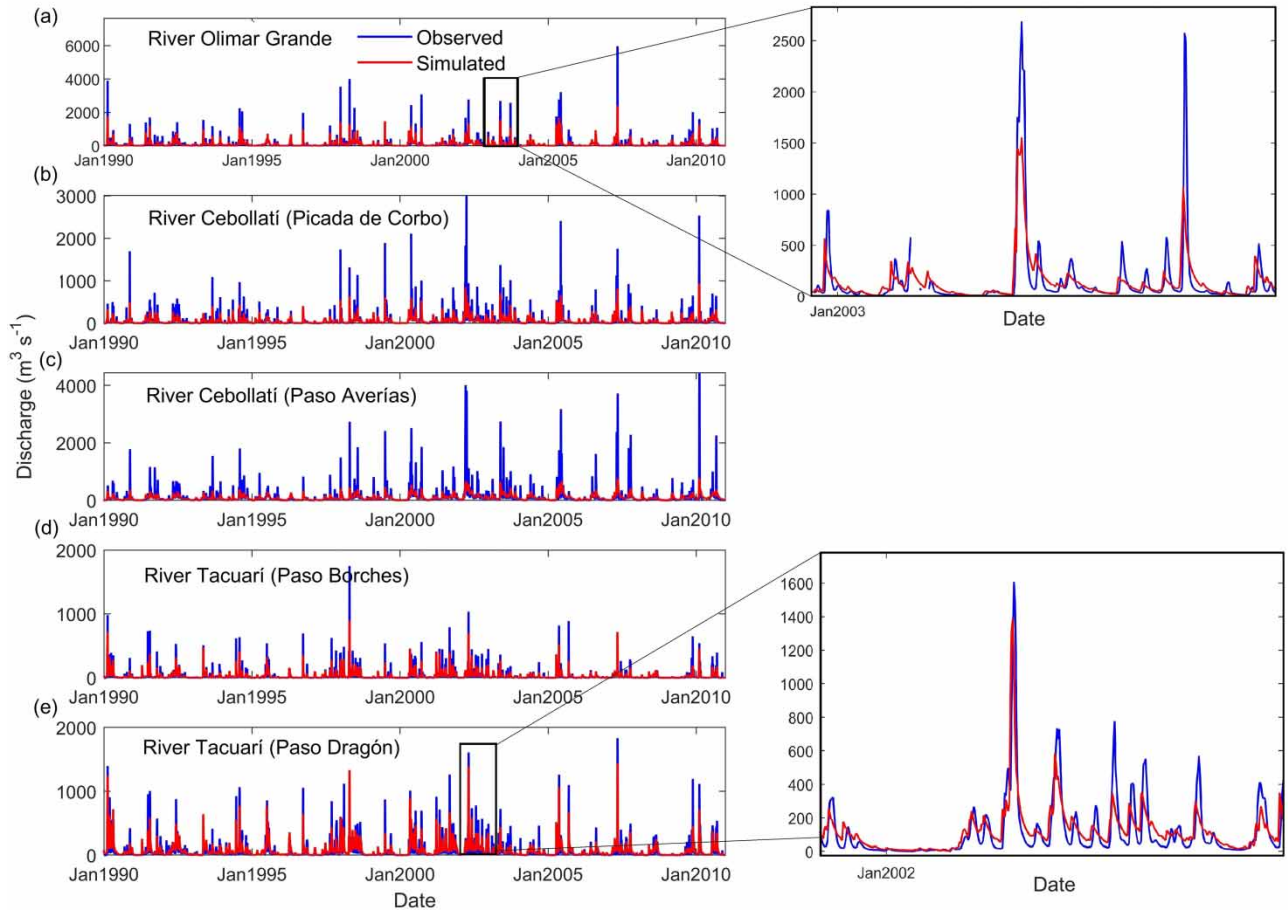


**Figure 5** | Observed and simulated hydrographs in the Olimar Grande, Cebollatí, and Tacuarí rivers.

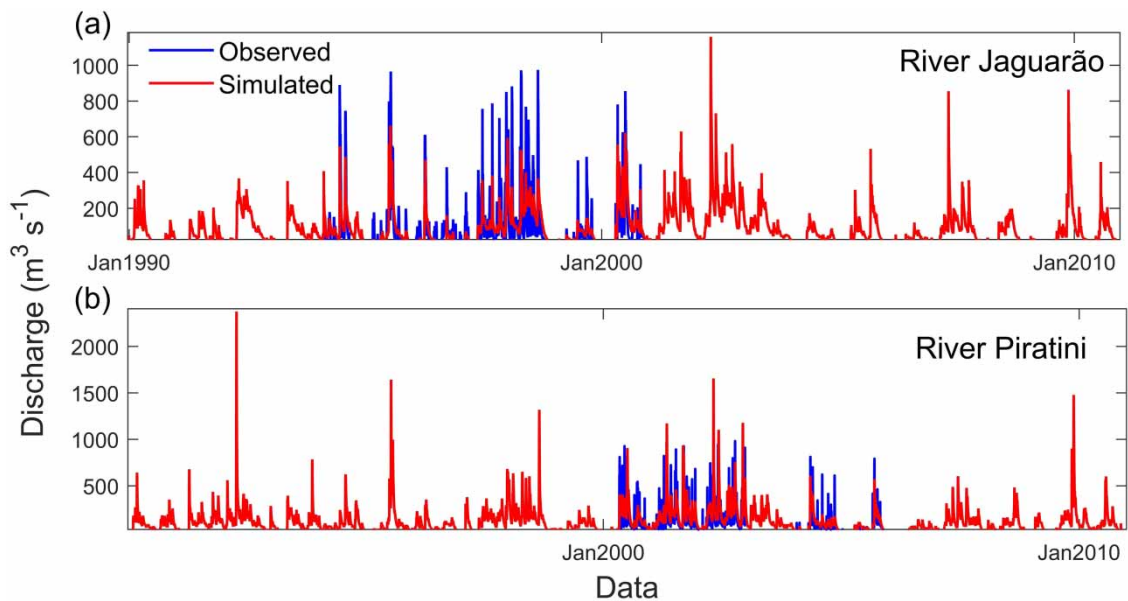


**Figure 6** | Observed and simulated hydrographs in Jaguarão and Piratini rivers.

**Table 1** | Performance metrics of the comparison between simulated and observed level anomalies at meteorological stations

| Gauges                  | NS    | NSlog | RMSE  |
|-------------------------|-------|-------|-------|
| Upstream sluice dam     | -0.02 | -1.70 | 0.43  |
| Downstream sluice dam   | -0.15 | -2.00 | 0.012 |
| Santa Izabel            | 0.72  | 0.41  | 0.47  |
| Santa Vitória do Palmar | 0.67  | 0.20  | 0.53  |
| Porto de Pelotas        | -0.22 | -0.08 | 0.32  |

oscillations occur in smaller time scales, within or between days, and are primarily caused by the wind (Möller *et al.* 1996, 2001). Therefore, the lack of wind data in the simulation with the MGB model was the main reason high frequencies were not modeled correctly, as also described by Lopes *et al.* (2018).

## Experiment 2

The quality of the results when including lateral connection between the minibasins at the lagoon are presented below. Firstly, different values were tested for the width of the fictional channel connecting the minibasins and the improvement on the results was evaluated through the performance metrics.

### Results of sensitivity tests to the width of the lateral connections

When comparing the performance metrics (NS and NSlog) of the simulated levels with different widths values of lateral connection with the results obtained previously in Experiment 1, we observe that the levels were better represented with the inclusion of the lateral connections (Tables 2 and 3). The best NS and NSlog values for each gauge are highlighted in bold in Tables 2 and 3.

For the stations upstream and downstream of the sluice dam, the best results of the metrics occurred when using widths of 10 m. The NS values for the gauges upstream and downstream of the sluice dam were 0.250 and 0.160, while the NSlog values

**Table 2** | NS for different widths of lateral connections

| Gauges                  | NS – Width of lateral connections (b) |        |        |        |        |        |               |               |
|-------------------------|---------------------------------------|--------|--------|--------|--------|--------|---------------|---------------|
|                         | 10 m                                  | 25 m   | 50 m   | 100 m  | 150 m  | 250 m  | 500 m         | 1,000 m       |
| Upstream sluice dam     | <b>0.250</b>                          | 0.234  | 0.215  | 0.184  | -0.022 | 0.121  | 0.059         | -0.010        |
| Downstream sluice dam   | <b>0.160</b>                          | 0.144  | 0.124  | 0.093  | -0.147 | 0.026  | -0.035        | -0.103        |
| Santa Izabel            | 0.656                                 | 0.669  | 0.685  | 0.725  | 0.600  | 0.736  | 0.757         | <b>0.773</b>  |
| Santa Vitória do Palmar | 0.779                                 | 0.793  | 0.807  | 0.822  | 0.664  | 0.837  | <b>0.841</b>  | 0.836         |
| Porto de Pelotas        | -0.192                                | -0.192 | -0.191 | -0.191 | -0.218 | -0.190 | <b>-0.189</b> | <b>-0.189</b> |

The best results among simulations with different lateral connections are highlighted in bold.

**Table 3** | NSlog for different widths of lateral connections

| Gauges                  | NSlog – Width of lateral connections (b) |        |        |               |        |        |              |              |
|-------------------------|--|--------|--------|---------------|--------|--------|--------------|--------------|
|                         | 10 m                                     | 25 m   | 50 m   | 100 m         | 150 m  | 250 m  | 500 m        | 1,000 m      |
| Upstream sluice dam     | <b>-0.181</b>                            | -0.203 | -0.228 | -0.268        | -1.699 | -0.346 | -0.417       | -0.480       |
| Downstream sluice dam   | <b>-0.468</b>                            | -0.491 | -0.518 | -0.559        | -2.003 | -0.642 | -0.715       | -0.778       |
| Santa Izabel            | 0.328                                    | 0.340  | 0.357  | 0.379         | -1.316 | 0.415  | 0.440        | <b>0.463</b> |
| Santa Vitória do Palmar | 0.663                                    | 0.695  | 0.724  | 0.753         | 0.199  | 0.783  | <b>0.792</b> | 0.790        |
| Porto de Pelotas        | -0.055                                   | -0.055 | -0.055 | <b>-0.053</b> | -0.078 | -0.054 | -0.054       | -0.055       |

The best results among simulations with different lateral connections are highlighted in bold.



were  $-0.181$  and  $-0.468$ , respectively. It is observed that the increase in width results in a worsening of the results, both for the coefficient NS and NSlog.

For the others, the best NS results were observed with widths of 500 and 1,000 m, which indicates that there was no single width that resulted in the best values for all gauges simultaneously. The NSlog metric had better values for the width of 1,000 m in the *Santa Isabel* gauge and 500 m in *Santa Vitória do Palmar*. However, for the Porto de Pelotas gauge, there was little difference for the analyzed metrics.

Therefore, as it was not possible to adopt multiple lateral connections widths, the width of 100 m was adopted as it represented the best overall increment for the metrics simulated at all gauges. The advantage of adopting this methodology lies in the possibility of simulating large basins with floodplains with a structure of a single hydrological–hydraulic model.

One of the main motivation for Experiment 3, with the inclusion of the contour condition at the SGC, was that there was not good results between the level simulated and observed data at the upstream and downstream sluice dam gauges as well as at the *Porto de Pelotas* gauge.

### Experiment 3

Besides the performance metrics, to evaluate the results of Experiment 3, we visually compared the flooded areas by the model with those captured by satellite images. The downstream conditions at the SGC where a constant slope of  $0.50 \text{ m km}^{-1}$ , a constant slope equivalent to the sea level, and the observed level data at the downstream sluice dam gauge.

#### Test results with the inclusion of the downstream condition

Three downstream conditions were evaluated in this study using the MGB model which resulted in the flooded areas presented in Figure 7. The results were extracted after a dry period, on March 24, 2005, and for a wet period, on March 27, 2002. The flooded areas generated by the MGB model were compared with Landsat 5 satellite images in the region of the SGC during a wet period on September 27, 2000 (Figure 7(b)) and with Landsat 8 images during a dry period on May 24, 2018 (Figure 7(a)). The difference between the comparison dates of simulation and satellite images is because there were no good images for the simulated period.

When comparing the results to the satellite images, we observed that the inundation was better represented by the model when the downstream condition of the sluice dam was used. In all situations, the flooded area was overestimated by the model during the dry period in the SGC region. Also, for all downstream conditions and periods, the model represented the flooded area of the Mirim Lagoon satisfactorily and within its limits. Through visual analysis, we verified a good representation of the lowland regions of the rivers Jaguarão, Tacuarí, and Cebollatí, which are considered the main tributaries of the Mirim Lagoon.

The performance metrics (NS, NSlog, and RMSE) of the anomalies of the simulated levels with the downstream condition of the sluice dam indicates a greater approximation between the simulation and observed data for the gauges upstream and downstream of the sluice dam and for the *Porto de Pelotas gauge* when compared with the simulations only with the lateral connections, with NS values reaching 0.84 and 0.99. However, in the *Santa Isabel* and *Santa Vitória do Palmar* gauges, the improvement was not as pronounced. There was also a great improvement of NSlog with the use of the downstream condition when compared with the previous simulations of Experiments 1 and 2 (Table 4). The use of the data near the sluice dam as a downstream boundary condition enabled the inclusion of the dam operation and the effects from the levels of the Patos Lagoon on the Mirim Lagoon through the SGC. The improvement on the metrics at the gauges far from the SGC indicates the great influence that the levels on the SGC have on the entire Mirim Lagoon.

### Experiment 4

The results of Experiment 4 were composed of cotagrams of the simulated levels with sub-daily and hourly wind and its evaluation through the performance metrics (NS, NSlog, and RMSE). Different values of wind friction coefficient were tested in the simulations to evaluate the one that would bring the best overall results.

#### Results of water levels simulated with the effects of the wind

The performance metrics obtained in the sensitivity test of the model to the wind friction coefficient,  $C_d$ , in the simulations with wind at sub-daily (S-DW) and hourly (HW) data are presented in Tables 5–7. In these tables, the best results among simulations with sub-daily and hourly data are highlighted in bold.

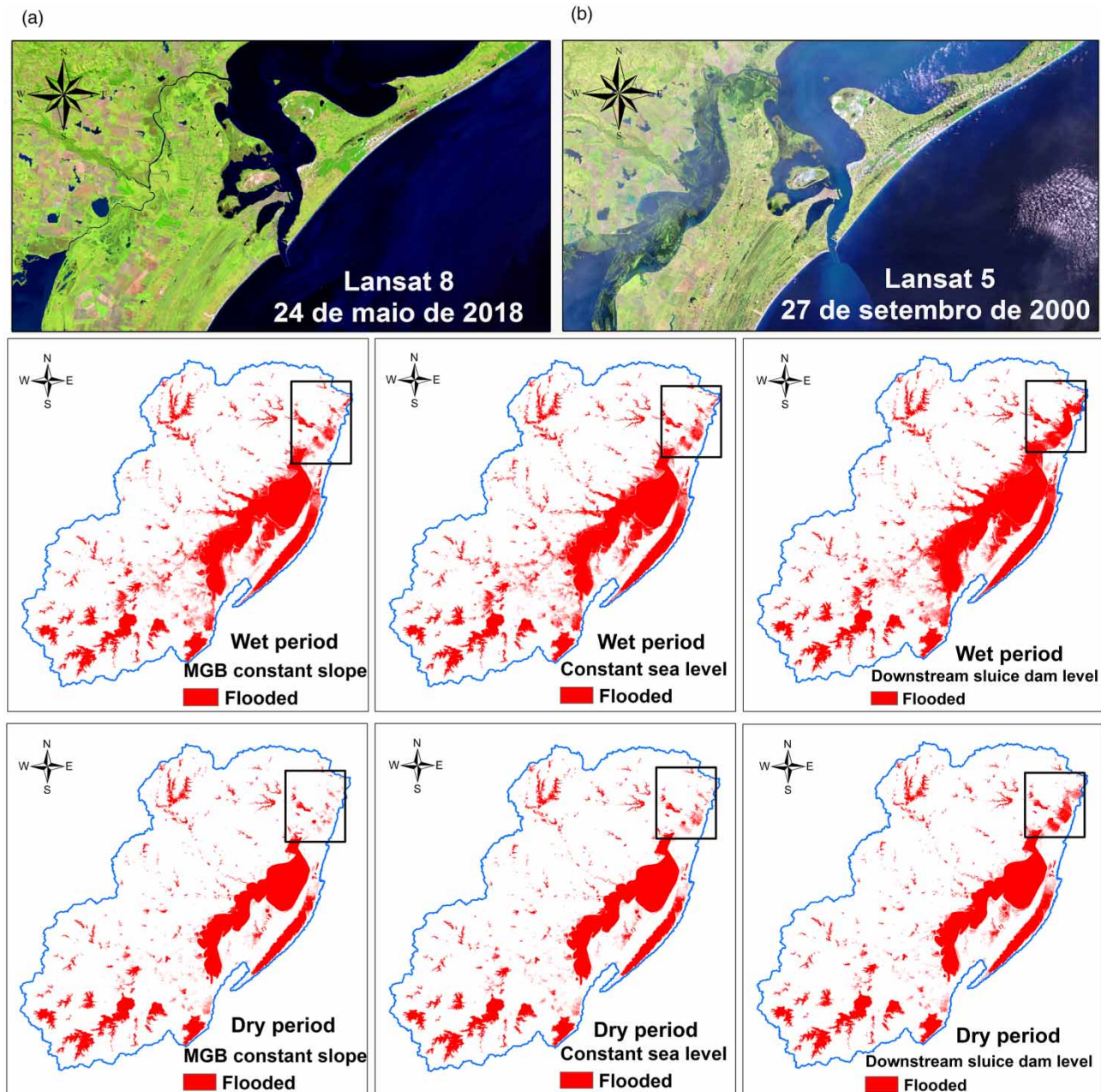


**Figure 7** | Comparison of the flooded area in the conditions of a constant slope of  $0.5 \text{ m km}^{-1}$ , a constant sea level, and the level of the dam-sluice measuring station downstream of the São Gonçalo channel on a wet period (b) and dry period (a) in Mirim Lagoon and its tributaries.

**Table 4** | Performance metrics of level anomalies with the downstream condition of the São Gonçalo canal dam-sluice

| Gauges                  | NS    | NSlog | RMSE  |
|-------------------------|-------|-------|-------|
| Upstream sluice dam     | 0.947 | 0.918 | 0.098 |
| Downstream sluice dam   | 0.999 | 0.999 | 0.012 |
| Santa Izabel            | 0.795 | 0.739 | 0.398 |
| Santa Vitória do Palmar | 0.846 | 0.812 | 0.358 |
| Porto de Pelotas        | 0.651 | 0.569 | 0.174 |

**Table 5** | NS results with daily and hourly wind data for values of  $C_d$  of  $2 \times 10^{-6}$ ,  $4 \times 10^{-6}$ ,  $10 \times 10^{-6}$ , and  $20 \times 10^{-6}$ 

| Gauges                  | Experiment 3 | $C_d (\times 10^{-6})$ |       |       |       |       |       |       |       |
|-------------------------|--------------|------------------------|-------|-------|-------|-------|-------|-------|-------|
|                         |              | 2                      |       | 4     |       | 10    |       | 20    |       |
|                         |              | S-DW                   | HW    | S-SW  | HW    | S-SW  | HW    | S-DW  | HW    |
| Upstream sluice dam     | 0.947        | <b>0.993</b>           | 0.946 | 0.992 | 0.945 | 0.992 | 0.944 | 0.991 | 0.941 |
| Downstream sluice dam   | 0.999        | <b>0.999</b>           | 0.999 | 0.999 | 0.999 | 0.998 | 0.998 | 0.997 | 0.995 |
| Santa Izabel            | 0.795        | <b>0.963</b>           | 0.822 | 0.962 | 0.821 | 0.960 | 0.800 | 0.957 | 0.769 |
| Santa Vitória do Palmar | 0.846        | <b>0.974</b>           | 0.852 | 0.973 | 0.853 | 0.971 | 0.839 | 0.967 | 0.796 |
| Porto de Pelotas        | 0.651        | <b>0.981</b>           | 0.800 | 0.980 | 0.799 | 0.980 | 0.770 | 0.978 | 0.709 |

The best results among simulations with sub-daily and hourly data are highlighted in bold.

**Table 6** | Results of NSlog against daily and hourly wind data for values of  $C_d$  of  $2 \times 10^{-6}$ ,  $4 \times 10^{-6}$ ,  $10 \times 10^{-6}$ , and  $20 \times 10^{-6}$ 

| Gauges                  | Experiment 3 | $C_d (\times 10^{-6})$ |       |       |       |       |              |       |       |
|-------------------------|--------------|------------------------|-------|-------|-------|-------|--------------|-------|-------|
|                         |              | 2                      |       | 4     |       | 10    |              | 20    |       |
|                         |              | S-DW                   | HW    | S-DW  | HW    | S-DW  | HW           | S-DW  | HW    |
| Upstream sluice dam     | 0.918        | <b>0.835</b>           | 0.836 | 0.834 | 0.835 | 0.832 | 0.835        | 0.829 | 0.833 |
| Downstream sluice dam   | 0.999        | <b>0.998</b>           | 0.998 | 0.998 | 0.998 | 0.998 | 0.998        | 0.996 | 0.996 |
| Santa Izabel            | 0.739        | <b>0.766</b>           | 0.762 | 0.765 | 0.760 | 0.748 | 0.752        | 0.727 | 0.737 |
| Santa Vitória do Palmar | 0.812        | 0.791                  | 0.790 | 0.790 | 0.791 | 0.765 | <b>0.793</b> | 0.727 | 0.786 |
| Porto de Pelotas        | 0.569        | <b>0.757</b>           | 0.756 | 0.756 | 0.754 | 0.748 | 0.744        | 0.725 | 0.713 |

The best results among simulations with sub-daily and hourly data are highlighted in bold.

**Table 7** | RMSE results regarding daily and hourly wind data for values of  $C_d$  of  $2 \times 10^{-6}$ ,  $4 \times 10^{-6}$ ,  $10 \times 10^{-6}$ , and  $20 \times 10^{-6}$ 

| Gauges                  | Experiment 3 | $C_d (\times 10^{-6})$ |              |       |       |       |       |       |       |
|-------------------------|--------------|------------------------|--------------|-------|-------|-------|-------|-------|-------|
|                         |              | 2                      |              | 4     |       | 10    |       | 20    |       |
|                         |              | S-DW                   | HW           | S-SW  | HW    | S-SW  | HW    | S-DW  | HW    |
| Upstream sluice dam     | 0.947        | <b>0.100</b>           | 0.101        | 0.101 | 0.101 | 0.102 | 0.101 | 0.104 | 0.102 |
| Downstream sluice dam   | 0.999        | <b>0.012</b>           | 0.013        | 0.013 | 0.013 | 0.015 | 0.014 | 0.019 | 0.018 |
| Santa Izabel            | 0.795        | 0.374                  | <b>0.373</b> | 0.376 | 0.375 | 0.386 | 0.381 | 0.401 | 0.395 |
| Santa Vitória do Palmar | 0.846        | 0.353                  | <b>0.351</b> | 0.355 | 0.351 | 0.369 | 0.353 | 0.397 | 0.367 |
| Porto de Pelotas        | 0.651        | <b>0.173</b>           | 0.174        | 0.174 | 0.174 | 0.175 | 0.175 | 0.178 | 0.179 |

The best results among simulations with sub-daily and hourly data are highlighted in bold.

These simulations were performed with the downstream condition of the sluice dam presented in Experiment 3 and with a lateral connection of 100 m width of the fictitious channel presented in Experiment 2. The tables also present the metrics obtained in Experiment 3 for comparison.

In general, results show that the friction coefficient of  $2 \times 10^{-6}$  resulted in the best performance metrics. The exception was the Santa Vitória do Palmar gauge, where the best performance for the NSlog metric was obtained using hourly wind data and a high  $C_d$  value of  $10 \times 10^{-6}$ .

Compared with the metrics obtained in the previous tests, significant improvement and excellent results were observed in the performance metrics in the model with the wind simulation and the downstream condition. This result demonstrates the great influence that wind has on the levels of the Mirim Lagoon and why it should not be neglected when possible.

In contrast to the modeling of the MSGb using sub-daily data, the inclusion of hourly information did not present a pronounced improvement. Note that the model presents flows and levels in daily time intervals, as well as the observed data, which may explain the reason why the greater discretization of wind information did not provide better results, in addition to the location of the gauges being different between hourly and sub-daily data.

It is also noticed a progressive decrease in the metrics values with the increase of the friction coefficient, using sub-daily or hourly data in the simulations. This decrease was more significant at Santa Isabel, Santa Vitória do Palmar, and Porto de Pelotas gauges. By using a  $C_d$  of  $2 \times 10^{-6}$  and with the inclusion of hourly wind data, there was an improvement in RMSE metrics, however, with a slightly higher performance.

Figure 8 shows the graphs of the simulated levels adjusted by the average of the observed data with the inclusion of the wind effect from sub-daily and hourly information, considering  $C_d$  equal to  $2 \times 10^{-6}$ , and the simulated levels in Experiment 2 (with only the lateral connections) and the observed data at each level station. The visual analysis indicates that the levels obtained from the simulation using sub-daily and hourly wind data were very similar, as the metrics showed.

We verified an improvement in the simulation including the wind, owing to the representation of the high-frequency oscillations in the levels, which were not possible without the inclusion of the wind effect. Despite the observed improvement, the amplitude of the simulated high-frequency oscillations was not as great as in some of the gauges, particularly the *Santa Isabel* and *Santa Vitória do Palmar gauges*. At the gauge downstream of the sluice dam at the SGC, the levels were practically identical between simulation and observation because these were used as a boundary condition.

The good results obtained in the present work with the MGB model show that it has potential for application in other locations and river-lagoon systems with similar characteristics, especially in large basins and where the wind plays a significant role on the observed levels. For the simulation of the analyzed system, the inclusion of the wind variable in the model proved to be very important for a better representation of the levels of Mirim Lagoon. At the same time, it is noteworthy that new studies in the region can be performed to be added to this one and help to understand, describe, and represent the dynamics of the region and its relationship with the local ecosystem.

Among some of the potential issues still to be explored in future studies, we can mention: testing of other sources and sets of wind data to explore their time availability, impacts, and possible improvements with their use; consider operating rules for the São Gonçalo sluice dam and incorporating them into the MGB model to better represent the exchanges between Mirim and Patos lagoons; and the inclusion of the various water uses in the basin, such as irrigation, to assess how these demands can influence the levels and flows in the lagoon.

## CONCLUSION

From this study, which applied the MGB for the Mirim-São Gonçalo transboundary basin, the following conclusions were drawn:

1. The inclusion of lateral connections between the minibasins located in the Mirim Lagoon caused a transfer of water between them, reducing the flow at the outlet of the MSGb and improving the simulation of water levels. With the inclusion of lateral connections, the NS values increased by 0.204, 0.243, 0.152, 0.005, and 0.03 in the gauges downstream and upstream of the sluice dam, Santa Vitória do Palmar gauge, Santa Isabel, and Porto de Pelotas, respectively. Moreover, the NSlog values increased by 1.441, 1.432, 0.553, 0.031, and 0.027 at these same gauges.
2. By inserting the levels observed at the limnimetric gauge of the sluice dam in the SGC as a downstream condition, we improved the simulated levels at the gauges in the channel itself and all others on the lagoon, demonstrating the influence of the Patos Lagoon on the levels in the Mirim Lagoon. The NS values increased from 0.2 to 0.9 at the stations downstream and upstream of the sluice dam, from 0.7 to 0.8 at the Santa Isabel and Santa Vitória do Palmar gauges, and from -0.191 to 0.7 at the Porto de Pelotas gauge. The NSlog values were also increased to between 0.7 and 0.9 at most limnimetric gauges.
3. The inclusion of the wind friction effect in the inertial flow propagation module of the MGB model benefited the representation of the simulated water levels in the MSGb. The best value of the wind friction coefficient  $C_d$  found in the sensitivity test was  $2 \times 10^{-6}$ . With the introduction of the wind in the simulation with a  $C_d$  of  $2 \times 10^{-6}$  and use of information from conventional sub-daily gauges, the anomalies of the simulated levels improved significantly when comparing to the observed levels, with results that can be considered excellent. All the limnimetric gauges around the basin had NS coefficients greater than 0.96 and NSlog of at least 0.76. With the use of hourly information from automatic stations, the same



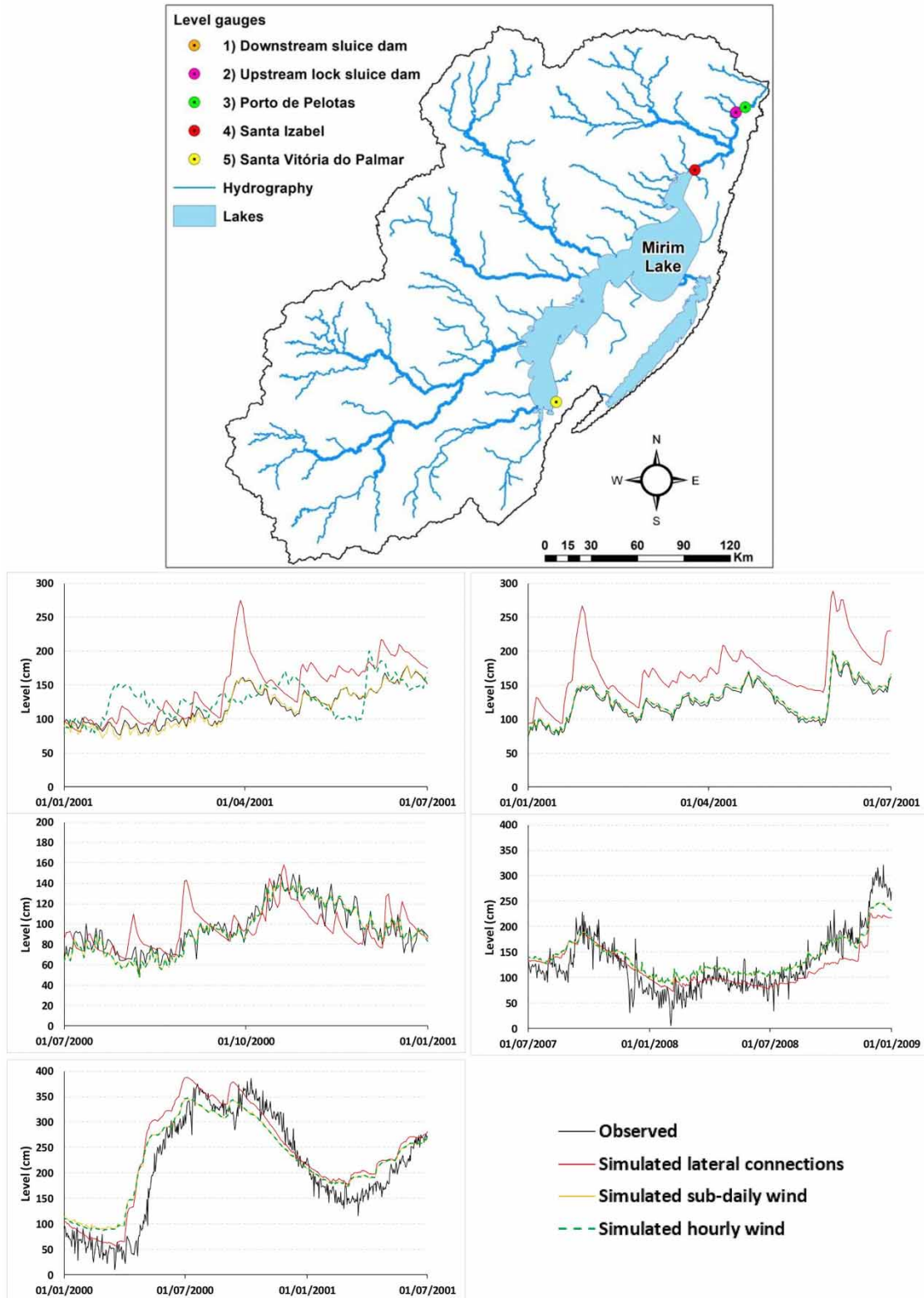


**Figure 8** | Plots of simulated anomalies with the inclusion of the effect of hourly and sub-daily wind and observed levels, considering  $C_d$  equal to  $2 \times 10^{-6}$ , at the level measuring stations.

result was not obtained, although, in some gauges, there was also improvement in the simulated levels. This can be attributed to the differences between the locations of the hourly and sub-daily wind gauges and also to the model presenting outputs in a daily time interval.

4. The MGB successfully simulated the water levels in the MSGb and demonstrated the importance of including the wind effect in hydrological models to represent the hydrodynamic processes of large lake environments, such as the region investigated in this study. The findings also improve the understanding on the hydrological dynamics of the Mirim Lagoon and the factors that govern its water levels and flow.

## ACKNOWLEDGEMENTS

The authors are grateful for the support provided by the Center for Teaching, Research and Extension in Hydrometry and Sediments for Watershed Management (<http://www.hidrosedi.com/>) of the Federal University of Pelotas (UFPEl) and the Large-Scale Hydrology Research Group of the Federal University of Rio Grande do Sul (UFRGS).

## DATA AVAILABILITY STATEMENT

All relevant data are included in the paper or its Supplementary Information.

## REFERENCES

- Abdelmoneim, H., Soliman, M. R. & Moghazy, H. M. 2020 Evaluation of TRMM 3B42V7 and chirps satellite precipitation products as an input for hydrological model over Eastern Nile basin. *Earth Systems and Environment* **4** (4), 685–698.
- Allen, R. G., Pereira, L. S., Raes, D. & Smith, M. 1998 Crop evapotranspiration: guidelines for computing crop water requirements. FAO Irrigation and Drainage Paper 56. FAO, Rome **300** (9), D05109.
- Amorim, P. B. & Chaffe, P. B. 2019 Towards a comprehensive characterization of evidence in synthesis assessments: the climate change impacts on the Brazilian water resources. *Climatic Change* **155** (1), 37–57.
- Barros, G. P., Marques, W. C. & Kirinus, E. P. 2014 Influence of the freshwater discharge on the hydrodynamics of Patos Lagoon, Brazil. *International Journal of Geosciences*. **5**, 925–942.
- Bates, P. D., Horritt, M. S. & Fewtrell, T. J. 2010 A simple inertial formulation of the shallow water equations for efficient two-dimensional flood inundation modelling. *Journal of Hydrology* **387** (1–2), 33–45.
- Brêda, J. P. L. F., de Paiva, R. C. D., Collischonn, W., Bravo, J. M., Siqueira, V. A. & Steinke, E. B. 2020 Climate change impacts on South American water balance from a continental-scale hydrological model driven by CMIP5 projections. *Climatic Change* **159** (4), 503–522.
- Cavalcante, R. B. L. & Mendes, C. A. B. 2014 Calibração e validação do módulo de correntologia do modelo IPH-A para a Laguna dos Patos (RS/Brazil). *Revista Brasileira de Recursos Hídricos* **19** (3), 191–204.
- Collischonn, W., Allasia, D., Da Silva, B. C. & Tucci, C. E. 2007 The MGB-IPH model for large-scale rainfall-runoff modelling. *Hydrological Sciences Journal* **52** (5), 878–895.
- Dargahi, B. & Setegn, S. G. 2011 Combined 3D hydrodynamic and watershed modelling of Lake Tana, Ethiopia. *Journal of Hydrology* **398** (1–2), 44–64.
- Fan, F. M. & Collischonn, W. 2014 Integration of the MGB-IPH model with geographic information system. *Brazilian Journal of Water Resources* **19** (1), 243–254.
- Fan, F. M., Pontes, P. R. M., Paiva, R. C. D. & Collischonn, W. 2014 Evaluation of a flood propagation method in rivers with inertial approximation of the Saint-Venant equations. *Revista Brasileira de Recursos Hídricos* **19** (4), 137–147.
- Fan, F. M., Buarque, D. C., Pontes, P. R. & Collischonn, W. 2015 A Map of Hydrologic Response Units for South America. XXI Simpósio Brasileiro de Recursos Hídricos, Brasília, DF.
- Fan, F. M., Collischonn, W., Quiroz, K. J., Sorribas, M. V., Buarque, D. C. & Siqueira, V. A. 2016 Flood forecasting on the Tocantins River using ensemble rainfall forecasts and real-time satellite rainfall estimates. *Journal of Flood Risk Management* **9** (3), 278–288.
- Farr, T. G., Rosen, P. A., Caro, E., Crippen, R., Duren, R., Hensley, S. & Alsdorf, D. 2007 The shuttle radar topography mission. *Reviews of Geophysics* **45** (2), 1–33.
- Fleischmann, A. S., Siqueira, V. A., Paris, A., Collischonn, W., Paiva, R. C. D., Pontes, P. R. M., Cretaux, J., Berge-N, M., Biancamaria, S. & Gossett, M. 2018 Modelling hydrologic and hydrodynamic processes in basins with large semi-arid wetlands. *Journal of Hydrology* **561**, 943–959.
- Fleischmann, A. S., Paiva, R. & Collischonn, W. 2019a Can regional to continental river hydrodynamic models be locally relevant? A cross-scale comparison. *Journal of Hydrology X* **3**, 100027.
- Fleischmann, A. S., Collischonn, W. & Paiva, R. C. D. 2019b Estimating design hydrographs at the basin scale: from event-based to continuous hydrological simulation. *Revista Brasileira de Recursos Hídricos* **24** (4), 1–10.
- Fragoso Jr., C. R., van Nes, E. H., Janse, J. H. & da Motta Marques, D. 2009 IPH-TRIM3D-PCLake: a three-dimensional complex dynamic model for subtropical aquatic ecosystems. *Environmental Modelling & Software* **24** (11), 1347–1348.

- Fragoso Jr., C. R., Marques, D. M. M., Ferreira, T. F., Janse, J. H. & van Nes, E. H. 2011 Potential effects of climate change and eutrophication on a large subtropical shallow lake. *Environmental Modelling & Software* **26** (11), 1337–1348.
- Gorgoglione, A., Crisci, M., Kayser, R. H., Chreties, C. & Collischonn, W. 2019 A new scenario-based framework for conflict resolution in water allocation in transboundary watersheds. *Water* **11** (6), 1174.
- Hartmann, C. & Harkot, P. F. G. 2018 Influence of São Gonçalo channel on sediment input to the Laguna dos Patos-RS estuary. *Brazilian Journal of Geosciences* **20** (1–4), 329–332.
- Hervouet, J. M. 2007 *Free Surface Flows: Modelling with the Finite Element Methods*. Wiley & Sons, England.
- Ji, Z. G. 2008 *Hydrodynamics and Water Quality: Modeling Rivers, Lakes and Estuaries*. John Wiley & Sons Inc, Hoboken, New Jersey.
- Kjerfve, B. 1986 Comparative oceanography of coastal lagoons. In: D. A. Wolfe (ed.). *Estuarine Variability*. Academic Press, New York, pp. 63–81.
- Komi, K., Neal, J., Trigg, M. A. & Diekkrüger, B. 2017 Modelling of flood hazard extent in data sparse areas: a case study of the Oti River basin, West Africa. *Journal of Hydrology: Regional Studies* **10**, 122–132.
- Kotzian, H. B. & Marques, D. M. 2004 Lagoa Mirim and the Ramsar convention: a model for transboundary action in water resources conservation. *Latin American Journal of Water Management* **1** (2), 101–111.
- Kundu, S., Khare, D. & Mondal, A. 2017 Past, present and future land use changes and their impact on water balance. *Journal of Environmental Management* **197**, 582–596.
- Kunz, J. G. & Castrogiovanni, A. C. 2020 Lagoa Mirim (Brasil/Uruguai): três versões turísticas de uma paisagem. *Revista Latino-Americana de Estudos em Cultura e Sociedade* **6** (1), 1–24.
- Li, Y., Zhang, Q., Yao, J., Werner, A. D. & Li, X. 2014 Hydrodynamic and hydrological modeling of the Poyang Lake catchment system in China. *Journal of Hydrologic Engineering* **19**, 607–616.
- Lian, Y., Chan, I., Singh, J., Demissie, M., Knapp, V. & Xie, H. 2007 Coupling of hydrologic and hydraulic models for the Illinois River Basin. *Journal of Hydrology* **344**, 210–222.
- Lopes, V. A. R., Fan, F. M., Pontes, P. R. M., Siqueira, V. A., Collischonn, W. & da Motta Marques, D. 2018 A first integrated modelling of a river-lagoon large-scale hydrological system for forecasting purposes. *Journal of Hydrology* **565**, 177–196.
- Marques, W. C. & Möller, O. O. 2008 Long-term temporal variability of river discharge and water levels in Lagoa dos Patos, Rio Grande do Sul, Brazil. *Revista Brasileira de Recursos Hídricos* **13** (3), 155–163.
- Möller, O. O., Stech, J. & Mata, M. M. 1996 The Patos Lagoon summertime circulation and dynamics. *Continental Shelf Research* **16** (3), 335–351.
- Möller, O. O., Castaing, P., Salomon, J. C. & Lazure, P. 2001 The influence of local and non-local forcing effects on the subtidal circulation of Patos Lagoon. *Estuaries* **24** (2), 297–311.
- Moriassi, D. N., Gitau, M. W., Pai, N. & Daggupati, P. 2015 Hydrologic and water quality models: performance measures and evaluation criteria. *Transactions of the ASABE* **58** (6), 1763–1785.
- Munar, A. M., Cavalcanti, J. R., Bravo, J. M., Fan, F. M., da Motta-Marques, D. & Fragoso Jr., C. R. 2018 Coupling large-scale hydrological and hydrodynamic modeling: toward a better comprehension of watershed-shallow lake processes. *Journal of Hydrology* **564**, 424–441.
- Nobre, A. D., Cuartas, L. A., Hodnett, M., Rennó, C. D., Rodrigues, G., Silveira, A. & Saleska, S. 2011 Height above the nearest drainage-a hydrologically relevant new terrain model. *Journal of Hydrology* **404** (1–2), 13–29.
- Oliveira, H. A. D., Fernandes, E. H. L., Moller, O. O. & Collares, G. L. 2015 Hydrological and hydrodynamic processes of Mirim Lagoon. *Revista Brasileira de Recursos Hídricos* **20** (1), 34–45.
- Oliveira, H., Fernandes, E., Möller, O. & García-Rodríguez, F. 2019 Relationships between wind effect, hydrodynamics and water level in the world's largest coastal lagoonal system. *Water* **11** (11), 2209.
- Paiva, R. C., Collischonn, W. & Tucci, C. E. 2011 Large scale hydrologic and hydrodynamic modeling using limited data and a GIS based approach. *Journal of Hydrology* **406** (3–4), 170–181.
- Paz, A. R., Collischonn, W., Risso, A. & Mendes, C. A. B. 2008 Errors in river lengths derived from raster digital elevation models. *Computers & Geosciences* **34** (11), 1584–1596.
- Paz, A. R., Bravo, J. M., Allasia, D., Collischonn, W. & Tucci, C. E. 2010 Large-scale hydrodynamic modeling of a complex river network and floodplains. *Journal of Hydrologic Engineering* **15** (2), 1–15.
- Pekel, J. F., Cottam, A., Gorelick, N. & Belward, A. S. 2016 High-resolution mapping of global surface water and its long-term changes. *Nature* **540** (7633), 418–422.
- Pinardi, M., Fenocchi, A., Giardino, C., Sibilla, S., Bartoli, M. & Bresciani, M. 2015 Assessing potential algal blooms in a shallow fluvial lake by combining hydrodynamic modelling and remote-sensed images. *Water* **7** (5), 1921–1942.
- Pontes, P. R. M., Fan, F. M., Fleischmann, A. S., de Paiva, R. C. D., Buarque, D. C., Siqueira, V. A., Jardim, P. F., Sorribas, M. V. & Collischonn, W. 2017 MGB-IPH model for hydrological and hydraulic simulation of large floodplain river systems coupled with open source GIS. *Environmental Modelling & Software* **94**, 1–20.
- Rennó, C. D., Nobre, A. D., Cuartas, L. A., Soares, J. V., Hodnett, M. G. & Tomasella, J. 2008 HAND, a new terrain descriptor using SRTM-DEM: mapping terra-firme rainforest environments in Amazonia. *Remote Sensing of Environment* **112** (9), 3469–3481.
- Schuster, R. C., Fan, F. M. & Collischonn, W. 2020 Scenarios of climate change effects in water availability within the Lagoon's basin. *Revista Brasileira de Recursos Hídricos* **25** (9), 1–15.

- Sharannya, T. M., Al-Ansari, N., Deb Barma, S. & Mahesha, A. 2020 Evaluation of satellite precipitation products in simulating streamflow in a humid tropical catchment of India using a semi-distributed hydrological model. *Water* **12** (9), 2400.
- Silva, D. V., Oleinik, P. H., Costi, J., de Paula Kirinus, E. & Marques, W. C. 2019 Residence time patterns of Mirim Lagoon (Brazil) derived from two-dimensional hydrodynamic simulations. *Environmental Earth Sciences* **78** (5), 1–11.
- Siqueira, V. A., Fleischmann, A., Jardim, P. F., Fan, F. M. & Collischonn, W. 2016 IPH-Hydro Tools: a GIS coupled tool for watershed topology acquisition in an open-source environment. *Brazilian Journal of Water Resources* **21** (1), 274–287.
- Siqueira, V. A., Paiva, R. C., Fleischmann, A. S., Fan, F. M., Ruhoff, A. L., Pontes, P. R., Paris, A., Calmant, S. & Collischonn, W. 2018 Toward continental hydrologic–hydrodynamic modeling in South America. *Hydrology and Earth System Sciences* **22** (9), 4815–4842.
- Sorribas, M. V., Paiva, R. C., Melack, J. M., Bravo, J. M., Jones, C., Carvalho, L., Beighley, E., Forsberg, B. & Costa, M. H. 2016 Projections of climate change effects on discharge and inundation in the Amazon basin. *Climatic Change* **136** (3), 555–570.
- Sosinski, L. T. W. 2009 Caracterização da Bacia Hidrográfica Mirim São Gonçalo e o uso dos recursos naturais. *Embrapa Clima Temperado- Documentos (INFOTECsilvaA-E)*.
- Valipour, M., Bateni, S. M. & Jun, C. 2021 Global surface temperature: a new insight. *Climate* **9** (5), 1–4.
- Vieira, E. F. 1988 *Planície Costeira do Rio Grande do Sul: Geografia física, vegetação e dinâmica sócio-demográfica*. Sagra Editora, Brasil, pp. 1–256.

First received 12 July 2021; accepted in revised form 15 October 2021. Available online 3 November 2021